Cell Metabolism
Article

Fast/Glycolytic Muscle Fiber Growth Reduces Fat Mass and Improves Metabolic Parameters in Obese Mice

Yasuhiro Izumiya,[1] Teresa Hopkins,[1] Carl Morris,[2] Kaori Sato,[1] Ling Zeng,[1] Jason Viereck,[3] James A. Hamilton,[3] Noriyuki Ouchi,[1] Nathan K. LeBrasseur,[2] and Kenneth Walsh[1,*]
[1]Molecular Cardiology, Whitaker Cardiovascular Institute
[2]Muscle and Aging Research Unit
[3]Department of Physiology and Biophysics
Boston University School of Medicine, Boston, MA 02118, USA
*Correspondence: kxwalsh@bu.edu
DOI 10.1016/j.cmet.2007.11.003

SUMMARY

In contrast to the well-established role of oxidative muscle fibers in regulating whole-body metabolism, little is known about the function of fast/glycolytic muscle fibers in these processes. Here, we generated a skeletal muscle-specific, conditional transgenic mouse expressing a constitutively active form of Akt1. Transgene activation led to muscle hypertrophy due to the growth of type IIb muscle fibers, which was accompanied by an increase in strength. *Akt1* transgene induction in diet-induced obese mice led to reductions in body weight and fat mass, resolution of hepatic steatosis, and improved metabolic parameters. Akt1-mediated skeletal muscle growth opposed the effects of a high-fat/high-sucrose diet on transcript expression patterns in the liver and increased hepatic fatty acid oxidation and ketone body production. Our findings indicate that an increase in fast/glycolytic muscle mass can result in the regression of obesity and metabolic improvement through its ability to alter fatty acid oxidation in remote tissues.

INTRODUCTION

The prevalence of metabolic disorders due to obesity is increasing in industrialized countries, leading to an increased risk for cardiovascular diseases (Reilly and Rader, 2003). It is widely held that exercise training confers improvements in whole-body metabolism. Conventional endurance exercise training elicits a variety of metabolic and morphological responses, including mitochondrial biogenesis (Zierath and Hawley, 2004), but does not induce muscle hypertrophy or hyperplasia or increase muscle force output (Hickson, 1980). Endurance training leads to an increase in the proportion of type I muscle fibers, also referred to as slow/oxidative fibers, which are high in mitochondrial content. Multiple lines of evidence indicate that type I muscle fibers play a pivotal role in glucose and lipid metabolism. For example, genetically altered mice that have more type I fibers exhibit resistance to diet-induced obesity (Wang et al., 2004), whereas mice that have reduced mitochondria and respiratory capacity in type I fibers develop abnormally increased body fat (Leone et al., 2005).

In contrast to endurance exercise, resistance exercise training is associated with an increase in protein synthesis and hypertrophy of type II fibers that are characterized as fast/glycolytic (Nader and Esser, 2001). This type of exercise promotes gains in maximal force output but has minimal effects on muscle fiber phenotype transformation (Williamson et al., 2001). Resistance training aimed at increasing type II muscle mass may also promote favorable effects on glucose metabolism, and this type of training is now recommended as a complementary exercise modality for insulin-resistant patients (Albright et al., 2000; American Diabetes Association, 2000). However, little is known about the mechanistic role that fast/glycolytic muscle fibers play in the development of obesity and obesity-related diseases.

The Akt family of serine/threonine protein kinases are functionally redundant signaling molecules that are activated by various extracellular stimuli through the phosphatidylinositol 3-kinase (PI3K) pathway. Numerous studies have implicated Akt1 signaling in the control of organ size and cellular hypertrophy (Shiojima and Walsh, 2006). Overexpression of constitutively active forms of Akt1 induces muscle hypertrophy both in vitro and in vivo (Bodine et al., 2001; Lai et al., 2004; Takahashi et al., 2002). In addition, overexpression of constitutively active Akt has been reported to promote fiber growth with no effect on fiber specification in regenerating skeletal muscle (Pallafacchina et al., 2002). Akt signaling in skeletal muscle is preferentially activated in response to resistance training, but not endurance training (Atherton et al., 2005; Bolster et al., 2003; Nader and Esser, 2001), suggesting that Akt signaling may function as a mediator of type II muscle hypertrophy.

To elucidate the role of fast/glycolytic muscle fibers in the control of obesity and obesity-related metabolism, we generated a conditional transgenic (TG) mouse that can reversibly grow functional type IIb muscle by switching Akt1 signaling on and off in a skeletal muscle-specific manner. We demonstrate that increases in fast/glycolytic muscle mass in obese mice lead to a reduction in accumulated white adipose tissue (WAT) and improvements in metabolic parameters independent of physical activity or changes in the level of food intake. These effects occur independently of muscle oxidative capacity and are associated with increases in fatty acid metabolism in liver.

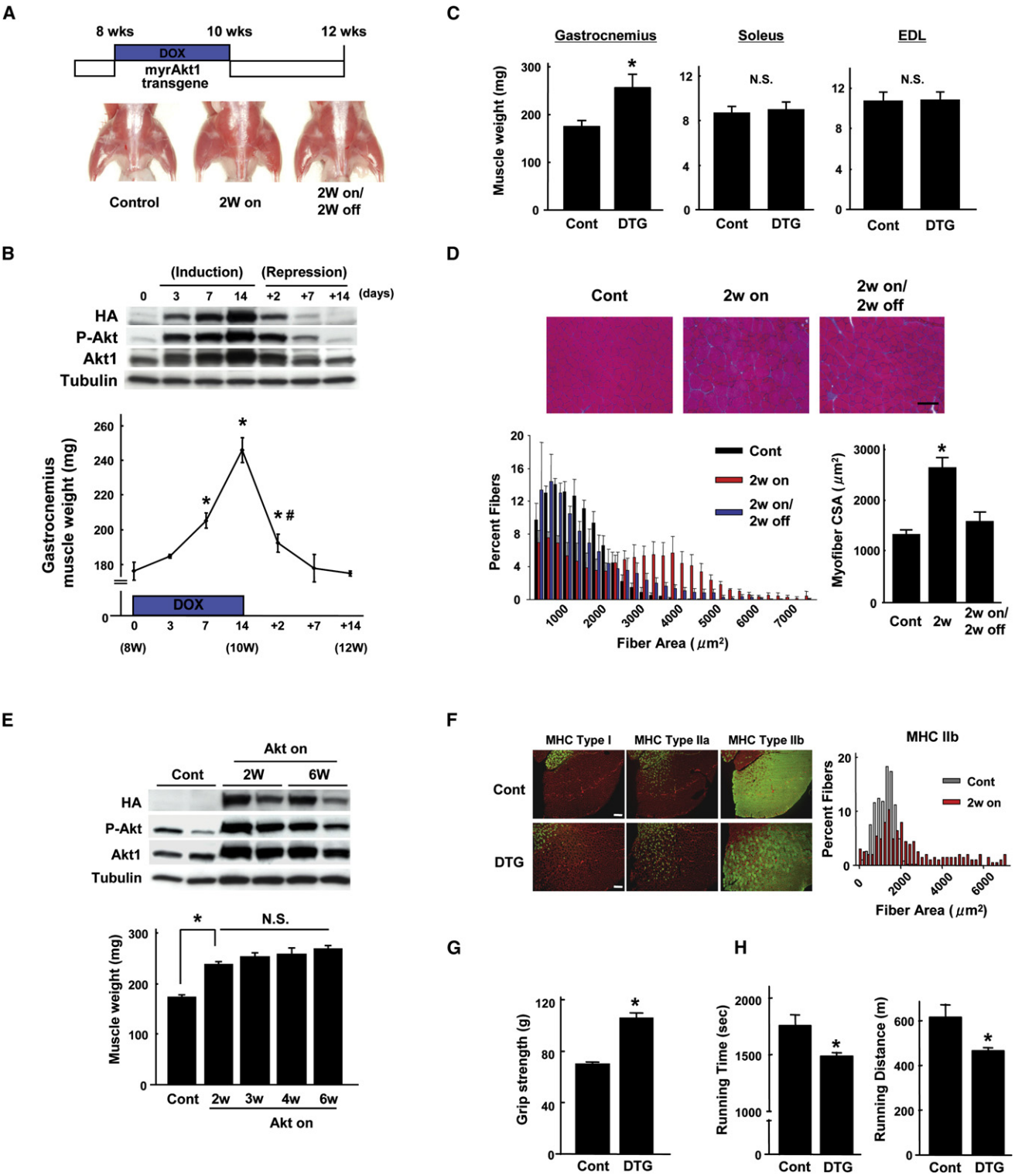

Figure 1. Conditional Activation of Akt1 in Skeletal Muscle Induces Reversible Type IIb Muscle Hypertrophy

(A) Top: schematic of doxycycline (DOX) treatment time course. Bottom: representative gross appearance of control and double-transgenic (DTG) mice after 2 weeks of transgene induction and after 2 weeks of induction followed by 2 weeks of repression. This experiment was initiated in DTG mice at 8 weeks of age.

(B) Top: time course of transgene expression following the addition of DOX (induction) and the subsequent removal of DOX (repression). Representative blots of gastrocnemius muscle are shown. Bottom: time course of gastrocnemius muscle weight changes resulting from transgene induction followed by repression (n = 4–12 in each group). *p < 0.05 versus day 0; #p < 0.05 versus day 14.

(C) Gastrocnemius, soleus, and extensor digitorum longus (EDL) muscle weight in control (Cont) and DTG mice at 2 weeks after Akt1 activation (n = 6 in each group).

RESULTS

Skeletal Muscle-Specific, Conditional *Akt1* Transgenic Mice

Two lines of TG mice, TRE-myrAkt1 and 1256 [3Emut] MCK-rtTA, were used to generate skeletal muscle-specific conditional *Akt1* TG mice (see Figure S1A available online). The TRE-myrAkt1 line harbors a constitutively active myristoylated form of Akt1 under the control of tetracycline-responsive element (TRE) (Shiojima et al., 2005). The 1256 [3Emut] MCK-rtTA line expresses the reverse tetracycline transactivator (rtTA), a fusion of the TRE-binding protein and the VP16 transactivation domain, from the 1256 [3Emut] MCK promoter (Grill et al., 2003). The promoter employed in this mouse line has three mutated E box motifs and shows a heterogeneous pattern of muscle-specific expression with little or no activity in type I (slow/oxidative) skeletal muscle or heart (Shield et al., 1996). Treatment of double-transgenic (DTG) mice harboring both transgenes with doxycycline (DOX) results in *myrAkt1* transgene expression because DOX associates with the rtTA and enables it to bind to the TRE. Withdrawal of DOX inhibits rtTA binding to the TRE and results in the repression of *myrAkt1* expression in skeletal muscle.

Mating of TRE-myrAkt1 mice and 1256 [3Emut] MCK-rtTA mice resulted in the generation of mice with four different genotypes (wild-type, TRE-myrAkt1 TG, 1256 [3Emut] MCK-rtTA TG, and DTG) at the expected frequencies. Mice were divided into DOX(−) and DOX(+) groups. The DOX(+) group was treated with normal water until the age of 8 weeks, followed by DOX treatment for 2 weeks, and the DOX(−) group was treated with normal water until the age of 10 weeks (Figure S1B). Western blot analysis of gastrocnemius muscle lysates harvested at 10 weeks of age revealed *Akt1* transgene expression in DTG mice treated with DOX, detected by immunoblotting for the hemagglutinin (HA) tag on the transgene. Transgene induction was associated with a marked increase in the phosphorylation of Akt at Ser473 and a moderate increase in total Akt1 protein levels (Figure S1B). As shown in Figure S1C, *Akt1* transgene expression was detected in gastrocnemius muscle, but not in heart, diaphragm, lung, liver, or kidney. Collectively, these data show that the transgene expression was tightly regulated by DOX in a skeletal muscle-specific manner. However, the transgene was not expressed in all subsets of skeletal muscle because of the specificity of the 1256 [3Emut] MCK promoter fragment (Grill et al., 2003). Transgene expression was detected in gastrocnemius and quadriceps muscle, which contain a mixture of fast and slow fibers but are composed predominantly of type II fibers. Transgene expression was not detected in soleus or extensor digitorum longus (EDL) muscles, which are classified as slow and fast, respectively (Figure S1D). Thus, the overall increase in whole-body skeletal muscle mass was relatively modest in this model. Finally, there was no difference in Akt2 expression levels or phosphorylation at residue Ser474 between control and DTG mice (Figure S2).

Akt1 Transgene Activation Promotes Type IIb Fiber Hypertrophy

To examine the phenotypic consequences of *Akt1* transgene expression, mice at 8 weeks of age were treated with DOX for 2 weeks. As shown in Figure 1A, activation of Akt1 signaling induced noticeable hindlimb muscle growth at the 2 week time point. Akt1-induced muscle growth could be reversed by the withdrawal of DOX from the drinking water for 2 weeks following 2 weeks of induction by DOX. The time course of transgene induction by DOX and repression by DOX withdrawal is shown in Figure 1B. Transgene expression increased in a time-dependent manner and correlated with an increase in gastrocnemius muscle mass (Figure 1B). Marked repression of transgene expression was observed as early as 2 days after withdrawal of DOX, and this corresponded to a dramatic regression of hypertrophy. By 7 days after DOX withdrawal, the gastrocnemius muscle mass returned to the basal levels observed in noninduced animals. Treatment with DOX for 2 weeks led to a 39% increase in gastrocnemius muscle but had no effect on soleus or EDL mass, consistent with the lack of transgene activation in these muscle groups (Figure 1C).

A subgroup of myofibers undergo reversible hypertrophy upon *Akt1* transgene activation and repression. Quantitative analysis of fiber size in histological sections of gastrocnemius muscle revealed that a portion of fibers undergo a reversible increase in cross-sectional area (CSA) (Figure 1D). While the extent of fiber growth was heterogeneous, the average CSA increased approximately 2-fold 2 weeks after Akt1 activation. Fiber size returned to that of the noninduced state within 2 weeks of transgene inactivation.

Maintaining transgene expression for 3, 4, or 6 weeks led to relatively smaller increases in skeletal muscle hypertrophy compared to the 2 week time point (Figure 1E), indicating the development of a plateau in the muscle growth process. Levels of *Akt1* transgene expression and levels of Akt phosphorylation were similar between the 2 and 6 week time points. Analysis of histological sections revealed that the increase in myofiber hypertrophy induced by prolonged Akt1 activation was not associated with detectable interstitial fibrosis or inflammation (data not shown).

Gastrocnemius muscle sections were stained with type I, IIa, or IIb myosin heavy chain (MHC) isoform antibodies to determine the fiber types that undergo hypertrophy. As shown in Figure 1F, type IIb fibers were markedly larger in DTG mice than in control mice. Quantitative analysis revealed that the average CSA of type IIb fibers increased from 1406 ± 21 μm^2 prior to transgene induction to 2788 ± 139 μm^2 following 2 weeks of transgene

(D) Histological analysis of myofiber growth. Top: hematoxylin and eosin (H&E) staining of gastrocnemius muscle sections. Scale bar = 100 μm. Bottom left: distribution of mean cross-sectional areas (CSAs) of muscle fibers. Bottom right: mean CSA of muscle fibers (n = 6 in each group).
(E) Top: western blot analysis of transgene expression after 2 and 6 weeks of DOX treatment. Bottom: gastrocnemius muscle weight at 2, 3, 4, and 6 weeks after DOX treatment (n = 6–12 in each group).
(F) Left: representative images of gastrocnemius muscle sections stained with MHC type I, IIa, or IIb antibody (green) and laminin (red) from control and DTG mice 2 weeks after Akt1 activation. Right: distribution of mean CSAs of type IIb muscle fibers from control and DTG mice after 2 weeks of DOX treatment.
(G) Forelimb grip strength of control mice and DTG mice after 2 weeks of DOX treatment (n = 6 in each group).
(H) Results of forced treadmill exercise test on MCK-rtTA single-TG control mice and DTG mice after 2 weeks of DOX treatment (n = 4 in each group).
Results are presented as mean ± SEM. *$p < 0.05$ versus control; N.S., not significant.

induction (n = 4 in each group, $p < 0.01$). In contrast, there was little or no increase in the CSA of the less abundant type I MHC-positive or type IIa MHC-positive fibers (Figure 1F and data not shown).

A series of physiological experiments were performed to assess the strength and treadmill performance of the DTG mice. Consistent with the *Akt1* transgene expression profile in type IIb fibers, the peak forelimb grip force of the DTG mice was about 50% greater than that of control mice 2 weeks after Akt1 induction (Figure 1G). On the other hand, a forced treadmill exercise test revealed that DTG mice exhibit a reduced capacity for running compared to control mice (Figure 1H). Impaired exercise capacity in DTG mice was manifest in a 15% decrease in exercise time and a corresponding 24% decrease in running distance. Calculation of work, a product of body weight, gravity, vertical speed, and time, revealed a 21% decrease in DTG mice (927.5 ± 89.5 J versus 731.5 ± 72.3 J). These results indicate that Akt1 activation in type IIb muscle fibers confers a "resistance exercise training" phenotype to mice.

Akt1-Mediated Muscle Hypertrophy Diminishes Fat Mass in Diet-Induced Obese Mice

To investigate the relationship between type II muscle growth and obesity-related metabolism, control and noninduced DTG mice were fed a high-fat/high-sucrose (HF/HS) diet for 8 weeks to induce weight gain. Thereafter, mice were provided DOX in their drinking water. Prior to transgene induction, DTG mice fed the HF/HS diet exhibited a progressive increase in overall body mass relative to mice fed normal chow. Induction of the *Akt1* transgene with DOX led to a decrease in overall body weight relative to control mice that were fed the HF/HS diet. A representative experiment is shown in Figure 2A. The reduction in overall body weight appeared to reach a plateau after 4 weeks of transgene induction. In contrast, DOX treatment had no effect on body mass in mice fed a normal chow diet.

DTG mice fed the HF/HS diet appeared noticeably leaner than control mice fed the same diet after 4 weeks of treatment with DOX (Figure 2B, left), and this was accompanied by a visible reduction in the amount of visceral fat (Figure 2B, right). As an alternative approach to analyze differences in fat, we performed magnetic resonance imaging (MRI) on live mice. The increase in adipose tissue mass induced by the HF/HS diet and its reduction following skeletal muscle-specific induction of the *Akt1* transgene could be observed in axial images (1 mm thick) of the torso above the kidneys (Figure 2C). In this plane of analysis, it can be seen that 4 weeks of muscle transgene induction led to an appreciable loss of adipose tissue, although this level of adipose mass was greater than that observed in animals fed a normal chow diet. Similarly, muscle transgene induction reduced adipose tissue mass in animals fed a normal diet.

Quantitative analysis of fat-pad mass revealed that the HF/HS diet led to an increase in inguinal and subcutaneous adipose weight (Figure 2D). Activation of the *Akt1* transgene in skeletal muscle resulted in 47% and 44% reductions in the mass of inguinal and subcutaneous fat pads, respectively. However, the reduction in adipose mass was partial in this model, and transgene-induced animals fed the HF/HS diet still had appreciably more adipose tissue mass than control animals. Similarly, muscle transgene induction in animals fed a normal chow diet led to a small but reproducible decrease in inguinal fat-pad mass, and there was a trend toward lower levels of subcutaneous fat (Figure 2D). This loss in fat mass under these conditions, in combination with the modest increase in total skeletal muscle mass, might explain why transgene induction does not lead to a change in overall body weight in normal chow-fed mice (Figure 2A). Dietary conditions did not affect the extent of transgene-induced gastrocnemius muscle growth (Figure 2D). Histology was performed on gastrocnemius muscle and inguinal fat pads (Figure 2E). Similar extents of transgene-induced myofiber hypertrophy were observed in mice fed normal and HF/HS diets. The HF/HS diet led to an enlargement in the size of white adipocytes in control mice, whereas muscle transgene induction led to the atrophy of enlarged white adipocytes.

Body Composition Changes Caused by Akt1-Mediated Muscle Growth Are Reversible and Blocked by Rapamycin

To examine whether the effects of Akt-mediated muscle growth on body mass are reversible, body weight was monitored weekly as DOX was administered to diet-induced obese mice for 5 weeks and then withdrawn for 5 weeks. A representative experiment is shown in Figure S3A. DOX-induced transgene activation in muscle led to a progressive decrease in body weight in mice fed the HF/HS diet. This reduction in body weight was reversed following DOX withdrawal. In contrast to findings in mice subjected to uninterrupted transgene activation (Figure 2D), no significant differences in inguinal or subcutaneous fat mass were observed between control mice and DTG mice after 5 weeks of transgene repression (Figure S3B). Therefore, the effect of muscle growth on adipose tissue is reversible in this model, and mice display accelerated fat deposition and body weight gains following transgene inactivation.

To assess whether myofiber hypertrophy is required for the reduction in adipose tissue mass in this model, control and DTG mice were treated with the mammalian target of rapamycin (mTOR) inhibitor rapamycin (2.0 mg/kg/day, intraperitoneally) or vehicle throughout the DOX treatment period. This compound inhibits Akt-enhanced protein synthesis and growth processes (Harris and Lawrence, 2003; Phung et al., 2006; Shiojima et al., 2005). In these assays, rapamycin did not affect the induction of the *Akt1* transgene or levels of phosphorylated Akt in gastrocnemius muscle (Figure S3C). However, the inhibition of mTOR signaling completely inhibited Akt1-mediated muscle growth and blocked the regression in fat mass in diet-induced obese mice (Figure S3D). This finding underscores the role of mTOR-dependent skeletal muscle hypertrophy in the reduction in fat mass in this model.

Muscle Hypertrophy Normalizes Metabolic Parameters in Diet-Induced Obese Mice

We next examined the effect of Akt1-mediated muscle growth on metabolic parameters at the 4 and 6 week time points after transgene activation. Blood glucose levels were significantly elevated in HF/HS-fed control mice, but not in HF/HS-fed mice following transgene induction (Figure 3A). In contrast, there were no differences in fasting blood glucose levels between the different experimental groups of animals (data not shown). Fasting serum

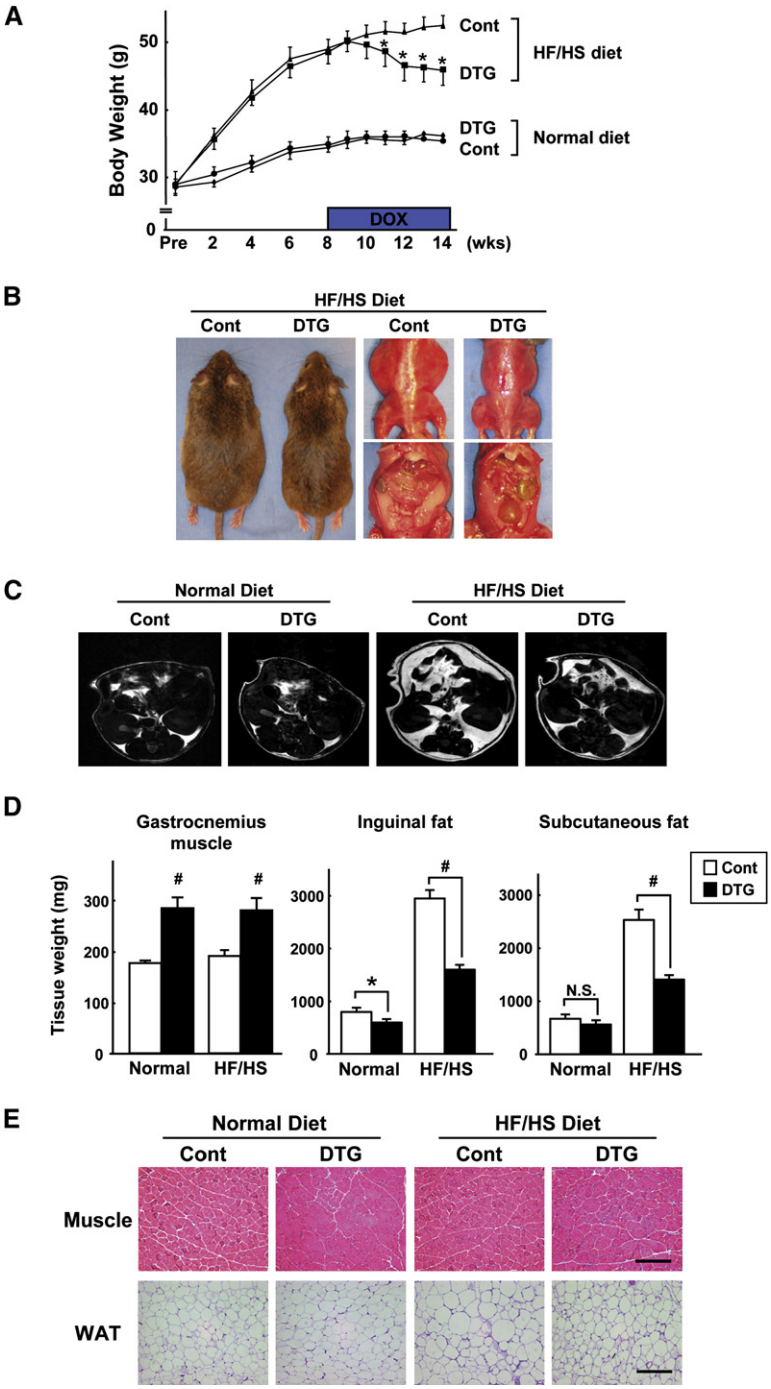

Figure 2. Akt1-Mediated Muscle Growth Reverses Diet-Induced Obesity

(A) Body weight of control and DTG mice fed a normal diet or a high-fat/high-sucrose (HF/HS) diet (n = 12 in each group). *p < 0.05 versus HF/HS-fed control mice.

(B) Representative gross appearance and ventral view of HF/HS-fed control and DTG mice at the 4 week time point of DOX treatment.

(C) Representative MRI images (1 mm axial slice) of each group of mice at the 4 week time point of DOX treatment, observed at the level of the right renal pelvis. Bright regions correspond to fat; dark regions represent lean body mass.

(D) Gastrocnemius muscle and inguinal and subcutaneous fat-pad weight in control and DTG mice after 6 weeks of DOX treatment (n = 12 in each group). *p < 0.05; #p < 0.01.

(E) Histological analysis of H&E-stained gastrocnemius muscle (top) and inguinal white adipose tissue (WAT, bottom) sections. Scale bars = 200 μm. MCK-rtTA single-transgenic mice were used as a control.

Results are presented as mean ± SEM.

insulin levels were significantly increased in control mice fed the HF/HS diet, but insulin levels were in the normal range in DTG mice fed the HF/HS diet. Akt1-mediated muscle hypertrophy was associated with an elevation of serum glucagon levels in the diet-induced obese mice. In contrast, obesity was associated with a marked elevation of serum leptin levels, and these levels decreased 84% under conditions of Akt1-mediated skeletal muscle hypertrophy. Serum levels of free fatty acids, triglycerides, and glycerol were not significantly different between the different experimental groups (Figure S4).

Glucose and insulin tolerance tests were performed on the different experimental groups of mice (Figure 3B). In contrast to control mice, DTG mice fed the HF/HS diet displayed normal glucose disposal rates. Similarly, the reduction in glucose due to insulin administration was impaired in control mice on the HF/HS diet compared to a normal diet, but Akt1 activation in muscle normalized the response to insulin administration. These results confirm that the HF/HS diet leads to an insulin-resistant state and reveal that these pathological effects can be reversed by Akt1-mediated muscle growth.

To examine glucose disposal in skeletal muscle, radiolabeled 2-deoxyglucose uptake into gastrocnemius muscle was assessed in vivo. Transgene induction led to 1.6- and 2.0-fold higher levels of glucose uptake in DTG mice fed normal and HF/HS diets, respectively (Figure 3C). Glucose uptake was greater in the DTG mice when normalized per milligram of gastrocnemius muscle, indicating that the increase in glucose disposal in DTG mice is not due solely to the increase in total muscle mass. Glucose uptake was significantly reduced in the WAT and heart of DTG mice (Figure S5). There were trends toward decreased glucose uptake in the liver, and in soleus and EDL muscle, which do not express the transgene. These data suggest that glucose utilization is restricted in tissues that do not express the transgene due to the glucose demands of the transgene-positive muscle. Finally, DTG mice displayed a statistically significant increase in serum lactate levels (Figure 3D), consistent with an increase in glucose utilization.

Muscle Growth Counteracts the Metabolic Consequences of Excess Adiposity

While a 4-week induction of the *Akt1* transgene in obese mice led to the normalization of metabolic parameters, these mice had

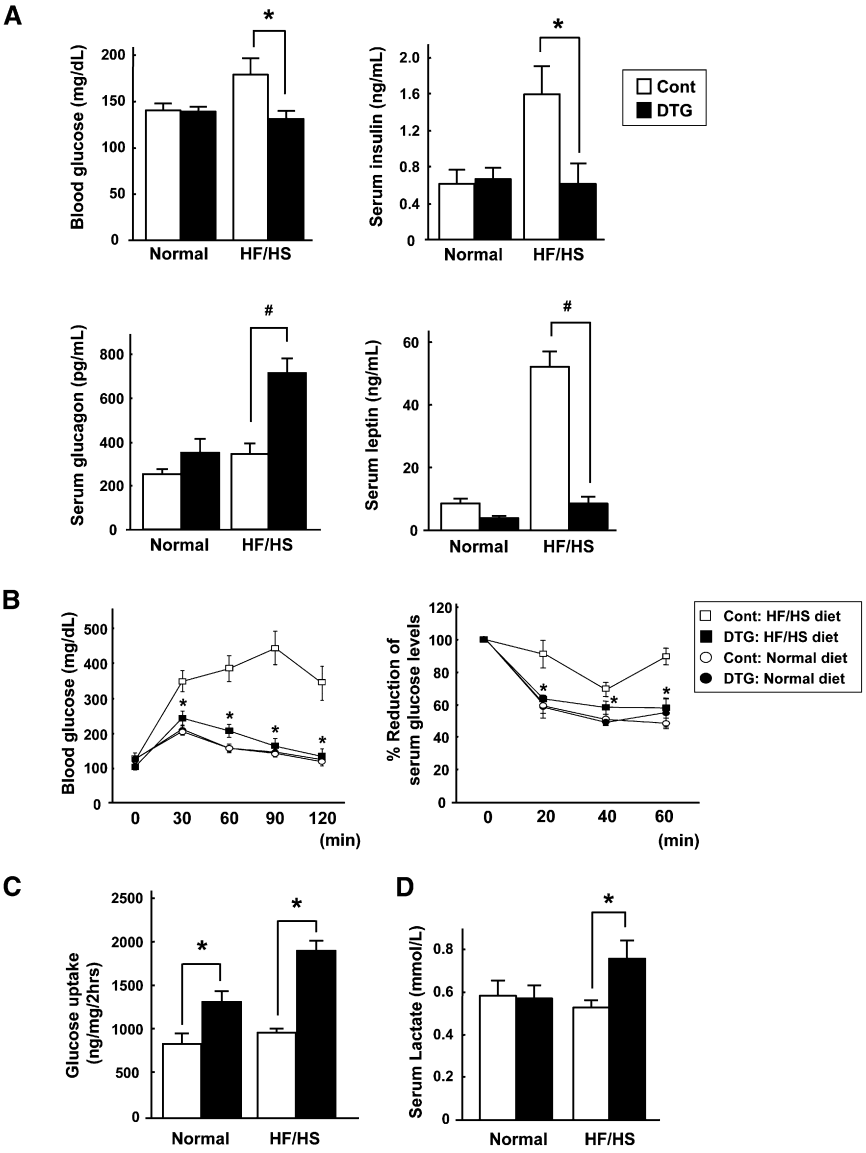

Figure 3. Akt1-Mediated Muscle Growth Normalizes Metabolic Parameters in Diet-Induced Obese Mice

(A) Blood glucose and serum insulin, glucagon, and leptin levels in normal or HF/HS-fed control and DTG mice after 6 weeks of DOX treatment (n = 7–12 in each group).

(B) Glucose (left) and insulin (right) tolerance tests in the different experimental groups of mice (n = 12 in each group). *p < 0.05 versus HF/HS-fed control mice.

(C) Glucose uptake into skeletal muscle in vivo (n = 6 in each group).

(D) Serum lactate levels in the different experimental groups of mice (n = 7 in each group). MCK-rtTA single-transgenic mice were used as a control.

Results are presented as mean ± SEM. *p < 0.05; #p < 0.01.

considerably higher levels of overall body weight and fat mass when compared to mice fed a normal diet (Figure 2). Thus, it was not clear whether the metabolic improvement in this model results from the reduction in fat mass per se or whether the Akt1-mediated muscle growth counteracts the pathological consequences of excess adiposity. To distinguish between these alternative explanations, fat mass and metabolic function were compared between control nontransgenic mice that had been fed the HF/HS diet for 4 weeks and transgene-induced mice that had been fed the HF/HS diet for 12 weeks. Mice in these two experimental groups were matched for body weight and fat mass (Figure 4A). Control mice fed the HF/HS diet for 4 weeks displayed an abnormal metabolic phenotype, indicated by impaired glucose clearance (Figure 4B), elevated leptin levels (Figure 4C), and hepatic steatosis (Figure 4D). In contrast, transgene-induced mice fed the HF/HS diet for 12 weeks displayed greater glucose disposal, lower leptin levels, and normal liver histology despite a fat mass equivalent to control mice fed the HF/HS diet for a shorter period. These results indicate that the Akt1-mediated increase in muscle mass can compensate for the excess adipose tissue, producing a normal metabolic phenotype in the overweight mice.

Effects of Akt1-Mediated Muscle Growth on Food Intake and Energy Expenditure

Control and DTG mice had similar caloric intakes on the HF/HS diet throughout the experimental period (Figure 5A). Control and DTG mice also displayed similar food intake levels on the normal chow diet, but the HF/HS diet led to a 1.8-fold increase in caloric intake in both strains of mice (data not shown). Ambulatory activity levels of control and DTG mice on the HF/HS diet were assessed by infrared beam interruption. Notably, the ambulatory activity of DTG mice was ~40% lower than that of control mice (Figure 5B). Despite this reduction in activity, analysis of whole-body O_2 consumption (VO_2) showed that energy expenditure was significantly higher in DTG mice compared to control mice on the HF/HS diet (Figure 5C). Furthermore, the respiratory exchange ratio (RER), which reflects the ratio of carbohydrate to fatty acid oxidation, was significantly lower in DTG mice, indicating that these mice used a relatively greater ratio of fatty acids as a fuel source. Collectively, these data show that the reductions in adipose mass that occur upon Akt1-mediated skeletal muscle growth are due at least in part to an increase in metabolic rate but are not the result of reductions in food intake or increased physical activity.

Akt1-Mediated Changes in Muscle Gene Expression

To assess the molecular mechanism by which Akt1-mediated muscle growth diminishes fat mass and normalizes metabolic parameters in diet-induced obese mice, whole-genome microarray and gene set analysis were performed on skeletal muscle

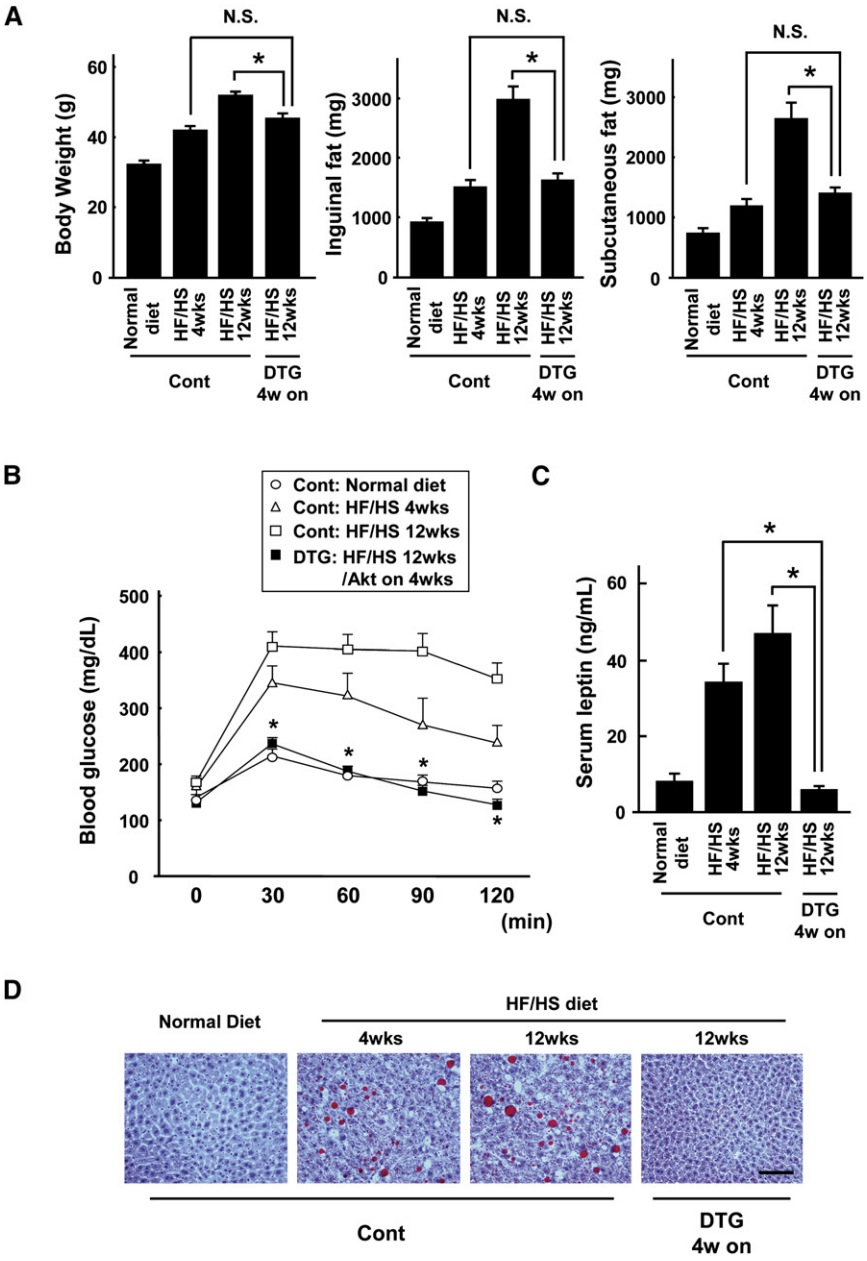

Figure 4. Akt1-Mediated Muscle Growth Counteracts the Metabolic Consequences of Excess Adiposity

(A) Body weight and inguinal and subcutaneous fat-pad weight in control and DTG mice fed a normal diet or a HF/HS diet for the indicated periods. DTG mice fed a HF/HS diet for 12 weeks and treated with DOX for 4 weeks (starting at the 8 week time point) had body weight and fat mass equivalent to control mice fed a HF/HS diet for 4 weeks.

(B) Glucose tolerance test results in the different experimental groups of mice.

(C) Serum leptin levels in the different experimental groups of mice.

(D) Representative sections of liver stained with oil red O. Scale bars = 100 μm. MCK-rtTA single-transgenic mice were used as a control.

Results are presented as mean ± SEM (n = 6–9 in each group). *p < 0.05; N.S., not significant.

samples from HF/HS-fed control and DTG mice at the 3 week time point after DOX treatment. In gastrocnemius muscle, 1704 genes (7.5% of all genes represented on the array) were upregulated and 1690 genes (7.5%) were downregulated in DTG mice compared to control mice ($p < 0.01$ and false discovery rate [FDR] < 0.05). To evaluate differences between functionally related gene groups, gene set enrichment analysis (GSEA) was employed. Among 1214 a priori defined gene sets, 276 sets (22.7%) were upregulated and 47 sets (3.9%) were downregulated in muscle of DTG mice compared with control mice. GSEA plots and segments of heat maps are shown in Figure 6A. The gene set "starch/sucrose metabolism," which contains transcripts involved in glycolysis, was upregulated in DTG mice compared with control mice. On the other hand, the gene sets "nuclear receptors," "fatty acid metabolism," and "oxidative phosphorylation" were markedly downregulated in muscle of DTG mice compared with control mice.

Some of the genes identified as up- or downregulated in the gene array study were validated by quantitative real-time PCR (qRT-PCR) analysis of transcripts. qRT-PCR analysis revealed that PGC-1α, PPARα, and PPARδ transcripts were decreased by 76%, 83%, and 67%, respectively, in gastrocnemius muscle 3 weeks after *Akt1* transgene induction (Figure 6B). qRT-PCR also revealed that transcripts for muscle-enriched glycolytic genes such as hexokinase 2 (HK2), phosphofructokinase (Pfk), and lactate dehydrogenase A (LDHA) were significantly upregulated. Quantitative immunoblot analysis also revealed reductions in PGC-1α, PPARα, and PPARδ protein expression (Figure 6C; Figure S7). These results suggest that activation of the *Akt1* transgene in the skeletal muscle of obese mice leads to the upregulation of glycolytic pathways, whereas oxidative pathways are decreased.

Finally, muscle levels of the IL-6 transcript and circulating levels of IL-6 protein were not influenced by muscle growth in this model (Figure S6). In contrast, myostatin mRNA levels in gastrocnemius muscle were reduced by 30% 3 weeks after *Akt1* transgene induction.

Muscle Growth Promotes Fatty Acid Metabolism in Liver

Because the liver is important in metabolic homeostasis, we performed microarray analysis to determine the effects of the HF/HS diet and Akt1-mediated muscle growth on transcript expression in hepatic tissue. In control mice, 635 genes (2.8%) were upregulated and 646 genes (2.8%) were downregulated in liver of mice on the HF/HS diet compared with the standard diet (CH/CN;

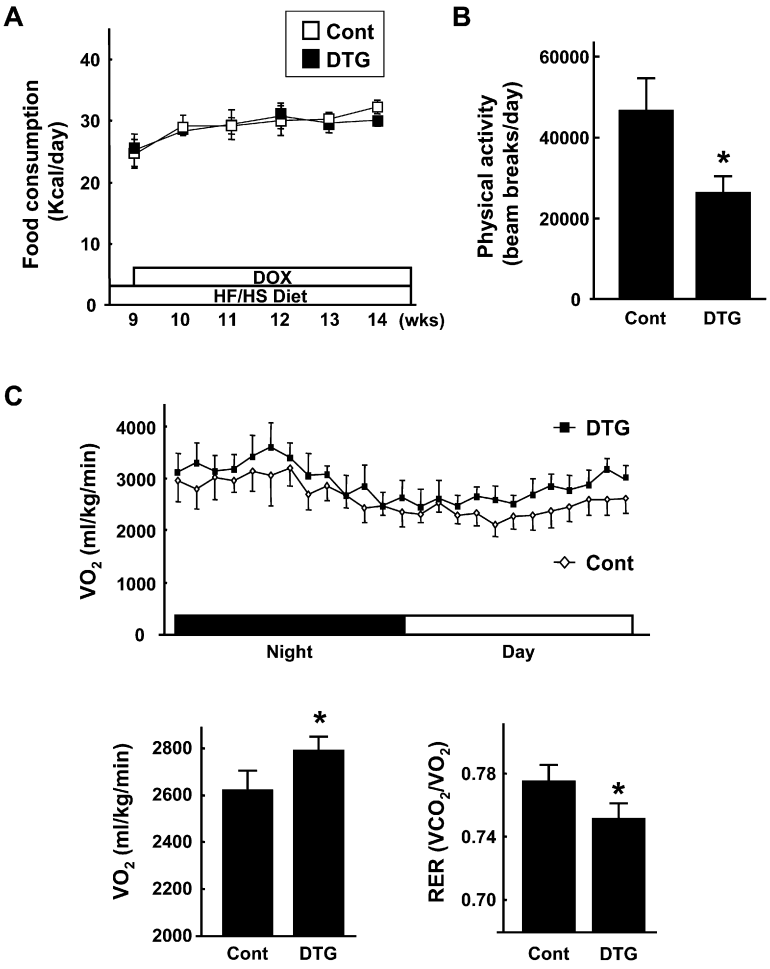

Figure 5. Akt1-Mediated Muscle Growth Has No Effect on Food Intake, Decreases Ambulatory Activity, and Increases Metabolic Rate

(A) Food consumption of control and DTG mice fed a HF/HS diet was monitored before and over 6 weeks of DOX treatment (n = 12 in each group).

(B) Ambulatory activity levels of control and DTG mice fed a HF/HS diet were determined by infrared beam interruption (n = 6 in each group).

(C) Top: trace of whole-body O_2 consumption (VO_2) determined using a metabolic measuring system for 24 hr in the absence of food in control and DTG mice 4 weeks after Akt1 activation (n = 6 in each group). Bottom left: average VO_2 in control and DTG mice fed a HF/HS diet. Bottom right: respiratory exchange ratio (RER) in control and DTG mice.

For all experiments, mice were fed a HF/HS diet for 8 weeks prior to DOX treatment. MCK-rtTA single-transgenic mice were used as a control. Results are presented as mean ± SEM. *p < 0.05.

Figure 7A, left column). Notably, Akt1-mediated skeletal muscle growth reversed the effects of the HF/HS diet on 861 (67%) of the 1281 transcript expression changes in liver (DH/CH; Figure 7A, right column). These results show that Akt1-mediated skeletal muscle growth can reverse the effects of a HF/HS diet on gene expression in liver, and they indicate that such alterations might be involved in the normalization of metabolic parameters in the diet-induced obese mice. qRT-PCR analysis on selected transcripts in these samples revealed that muscle growth is associated with increases in phosphoenolpyruvate carboxykinase (PEPCK) and glucose 6-phosphatase (G6Pase), which are involved in gluconeogenesis, and PGC-1α, carnitine palmitoyltransferase 1 (CPT1), and hepatocyte nuclear factor 4α (HNF4α), which are involved in fatty acid metabolism (Figure 7B). Akt1-mediated muscle growth in obese mice also led to a marked downregulation of mRNA for stearoyl-CoA desaturase 1 (SCD1), which catalyzes the conversion of saturated fatty acids to monosaturated fatty acids and is an important regulator of energy expenditure and body fat (Dobrzyn and Ntambi, 2005).

Consistent with the transcript profile data, livers excised from DTG mice displayed greater rates of fatty acid β-oxidation, and this effect was more pronounced in mice on the HF/HS diet (Figure 7C). Furthermore, ketone body levels, an indirect marker of hepatic fatty acid oxidation, were markedly increased in the serum and urine of DTG mice, particularly on the HF/HS diet (Figure 7D). Collectively, these data indicate that Akt1-mediated fast/glycolytic muscle growth leads to increased rates of fatty acid utilization in liver.

DISCUSSION

In the present study, we show that Akt1-mediated growth of muscle can regress obesity and resolve metabolic disorders in obese mice. Muscle-specific *Akt1* transgene expression led to hypertrophy of fast/glycolytic muscle fibers that was accompanied by atrophy of visceral adipocytes and regression of hepatic steatosis in diet-induced obese mice. Akt1-mediated muscle growth in obese mice also led to improved insulin sensitivity and reductions in blood glucose, insulin, and leptin levels. These effects occurred despite a reduction in physical activity following transgene induction and were achieved with no changes in food intake.

Accumulating evidence indicates that the Akt1 signaling pathway plays an important role in skeletal muscle hypertrophy in vitro (Bodine et al., 2001; Pallafacchina et al., 2002; Rommel et al., 2001; Takahashi et al., 2002). Previously, Lai et al. (2004) demonstrated that skeletal muscle-specific *Akt1* transgenic mice exhibit robust muscle growth, but the functional and physiological aspects of this muscle growth were not examined. In the present study, DOX-inducible *Akt1* transgene expression under the control of the 1256 [3Emut] MCK promoter fragment led to the hypertrophy of type IIb, but not I or IIa, muscle fibers. Transgene expression and fiber hypertrophy were detected in some but not all skeletal muscle tissues, likely due to the heterogeneous pattern of transgene expression from the MCK promoter fragment (Grill et al., 2003). Muscle hypertrophy in this model was reversible, and myofibers regressed to their noninduced size when DOX was removed from the drinking water. Activation of the *Akt1* transgene led to an increase in grip strength but a reduction in endurance on a treadmill test. Transcript profiling of skeletal muscle showed that transgene activation led to the induction of genes involved in glycolysis but decreased expression of genes associated with mitochondrial biogenesis and fatty acid

oxidation. Furthermore, *Akt1* transgene-induced muscle growth led to an increase in glucose uptake in muscle and an increase in circulating levels of lactate, indicative of Cori cycle activity. The increase in glucose uptake occurred in the absence of detectable Akt2 activation, and these findings are in contrast to those reported previously by Cleasby et al. (2007). Collectively, these data indicate that *Akt1* transgene expression promotes the growth of muscle that can be characterized as glycolytic/fast rather than oxidative/slow.

Using the inducible transgenic system, we show that Akt1-mediated hypertrophy of fast/glycolytic muscle fibers results in the regression of fat mass and improved metabolic homeostasis in mice that had previously been made obese through a high-calorie diet. These reductions in fat mass were reversible. Transgene inactivation led to a regression of muscle hypertrophy that was associated with accelerated gains in fat deposition and overall body weight, and large increases in circulating leptin and insulin levels indicating metabolic dysfunction. Moreover, rapamycin treatment blocked Akt1-mediated muscle hypertrophy and its salutary effects on body composition. The growth of fast/glycolytic muscle in obese mice also reversed hepatic steatosis, normalized responses to exogenously administered glucose and insulin, and lowered circulating levels of glucose, insulin, and leptin. These data illustrate the importance of fast/glycolytic muscle in the control of obesity and whole-body metabolism. The metabolic improvements were observed between 4 and 6 weeks after transgene activation, when the increase in muscle mass had stabilized. Thus, this model probably reflects the metabolic regulation that is associated with the maintenance phase of a strength training program rather than the initial period of muscle growth.

In contrast to the model described here, a number of studies have focused on the role of oxidative muscle fibers in metabolic homeostasis using mice that chronically express UCP1 (Li et al., 2000), calcineurin (Ryder et al., 2003), or PPARδ (Luquet et al., 2003; Wang et al., 2004) transgenes from skeletal muscle-specific promoters. For example, *PPARδ* transgenic mice display higher levels of type I fibers relative to type II fibers, increased running performance, and resistance to diet-induced obesity. Conversely, mice that are deficient in PGC-1α display abnormal oxidative fiber growth and develop an increase in body fat (Leone et al., 2005). These studies indicate that an increase in the "energy burn" in muscle can protect against weight gain and metabolic dysfunction. In addition, myostatin-deficient mice are resistant to diet-induced obesity (McPherron and Lee, 2002), but it is not clear whether this metabolic effect results from changes in type I or type II fibers or from the action of myostatin on adipose tissue (Feldman et al., 2006).

In the present study, we show that Akt1-mediated type II muscle fiber growth leads to an increase in whole-body energy expenditure in obese mice independent of physical activity levels. Transgene-induced changes in energy balance are indicated by an increase in circulating glucagon levels and the production of ketone bodies. Akt1-mediated muscle growth in obese mice also led to a marked decrease in circulating levels of leptin, which serves as an indicator of energy stores. The metabolic changes in the *Akt1* transgenic mice probably result from increased energy expenditure as a consequence of building and maintaining additional myofibrillar structures. Empirical data show that energy expenditure corresponds to the 3/4 power of lean body mass (Reitman, 2002). However, the overall increase in muscle mass was relatively small in the *Akt1* transgenic mice, and no statistically significant increase in body mass occurred as a result of transgene induction in animals fed a normal chow diet. In contrast, myostatin-deficient mice exhibit large increases in skeletal muscle mass throughout the body, leading to a doubling of body weight (McPherron et al., 1997). Thus, the results from the current study indicate that modest increases in type IIb skeletal muscle mass can have a profound systemic effect on whole-body metabolism and adipose mass.

Akt1-mediated growth of fast/glycolytic muscle in obese mice increases whole-body oxygen consumption, consistent with an increase in energy expenditure. Furthermore, these mice displayed a reduction in the respiratory exchange ratio, which reflects an increase in fatty acid β-oxidation. However, we could detect no increase in fatty acid oxidation in gastrocnemius muscle following transgene induction in obese or normal chow-fed mice (data not shown). In contrast, an increase in fatty acid oxidation could be observed in livers excised from these mice. Fat redistribution from adipose tissue to the liver is one of the features of obesity, and hepatic lipid deposition leads to insulin resistance and contributes to the pathogenesis of type 2 diabetes (Browning and Horton, 2004). Our study found that diet-induced hepatic steatosis was dramatically resolved following transgene-induced growth of type II muscle, indicating that the role of the liver was converted from lipid storage to lipid oxidation. Transcript profile analysis showed that an increase in fast/glycolytic fiber growth had numerous effects on hepatic metabolism. Muscle growth increased the expression of genes specifically associated with fatty acid oxidation and mitochondrial biogenesis and reversed the effects of the high-calorie diet on 67% of the 1281 transcript expression changes in liver. Akt1-mediated muscle growth led to a reduction in the hepatic expression of SCD1, which catalyzes the conversion of saturated fatty acids to monosaturated fatty acids and is an important target of leptin action (Cohen et al., 2002). The phenotype of the SCD1-deficient mouse is similar to that seen following Akt1-mediated skeletal muscle growth in obese mice. Both are lean and hypermetabolic and display reduced hepatic steatosis. Thus, the metabolic improvement resulting from type II skeletal muscle growth may be partly due to the downregulation of hepatic SCD1.

Our study found that an increase in fast/glycolytic muscle appeared to increase the animal's tolerance to excess adiposity. While Akt1-mediated skeletal muscle growth in mice fed the high-calorie diet resulted in a reduction in fat-pad mass, these animals retained significantly more adipose tissue than control animals on a normal chow diet, although they appeared metabolically normal and free of hepatic steatosis. To investigate this issue in greater detail, control mice were assessed after being fed the high-calorie diet for a shorter 4-week period. These mice displayed abnormal liver histology, insulin resistance, and markedly elevated leptin levels although they were matched in body weight and fat mass to mice fed the high-calorie diet for 12 weeks with 4 weeks of muscle transgene induction. These data indicate that the metabolic improvement observed following transgene induction is not the result of fat reduction per se, but that the increased type II muscle mass attenuates the pathological consequences of excess adiposity on whole-body metabolism. The metabolic improvement in this model may result

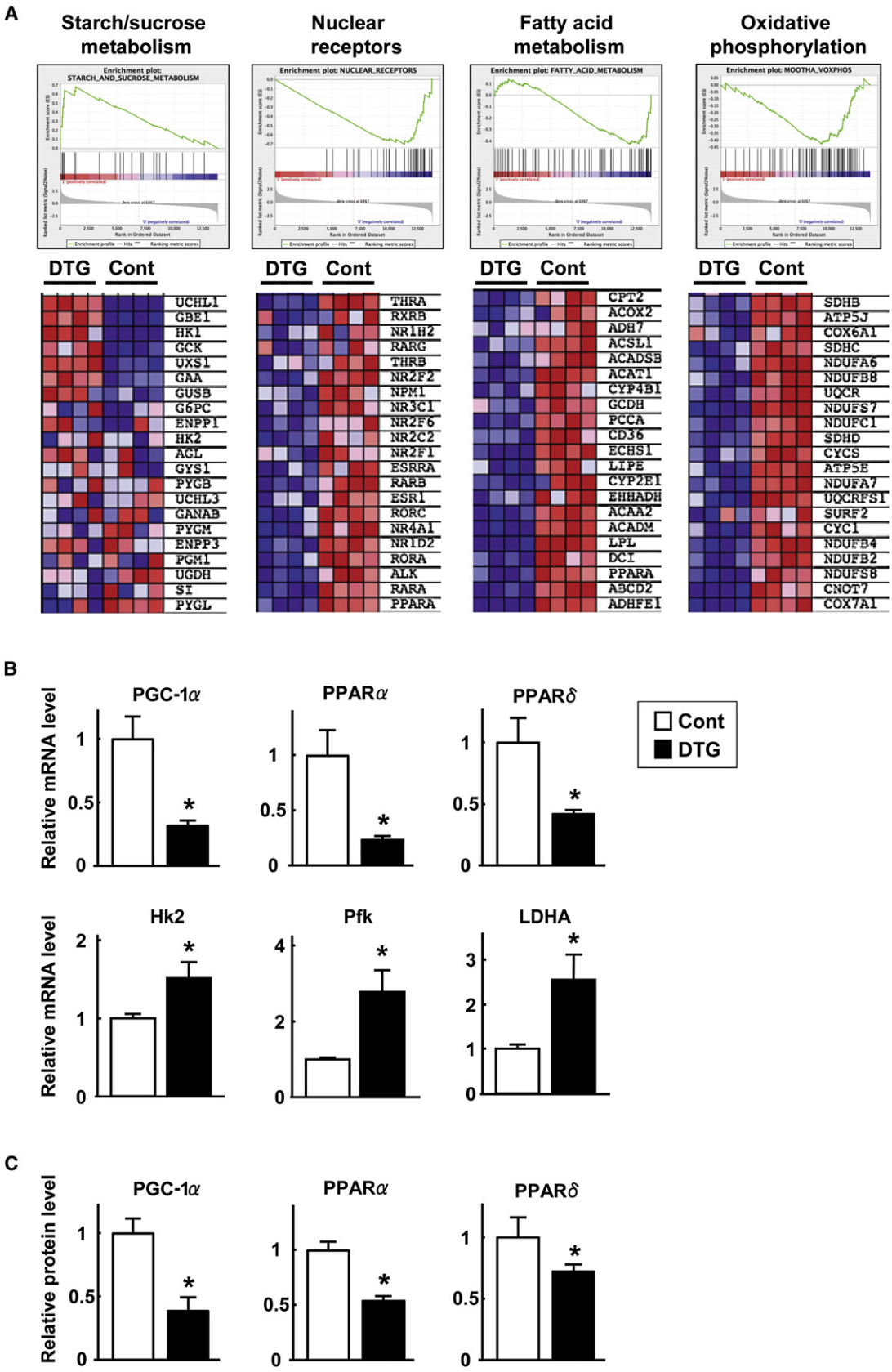
A
Starch/sucrose metabolism
Nuclear receptors
Fatty acid metabolism
Oxidative phosphorylation
DTG Cont
UCHL1 GBE1 HK1 GCK UXS1 GAA GUSB G6PC ENPP1 HK2 AGL GYS1 PYGB UCHL3 GANAB PYGM ENPP3 PGM1 UGDH SI PYGL
THRA RXRB NR1H2 RARG THRB NR2F2 NPM1 NR3C1 NR2F6 NR2C2 NR2F1 ESRRA RARB ESR1 RORC NR4A1 NR1D2 RORA ALK RARA PPARA
CPT2 ACOX2 ADH7 ACSL1 ACADSB ACAT1 CYP4B1 GCDH PCCA CD36 ECHS1 LIPE CYP2E1 EHHADH ACAA2 ACADM LPL DCI PPARA ABCD2 ADHFE1
SDHB ATP5J COX6A1 SDHC NDUFA6 NDUFB8 UQCR NDUFS7 NDUFC1 SDHD CYCS ATP5E NDUFA7 UQCRFS1 SURF2 CYC1 NDUFB4 NDUFB2 NDUFS8 CNOT7 COX7A1
B
Relative mRNA level
PGC-1α
PPARα
PPARδ
Cont
DTG
Hk2
Pfk
LDHA
C
Relative protein level

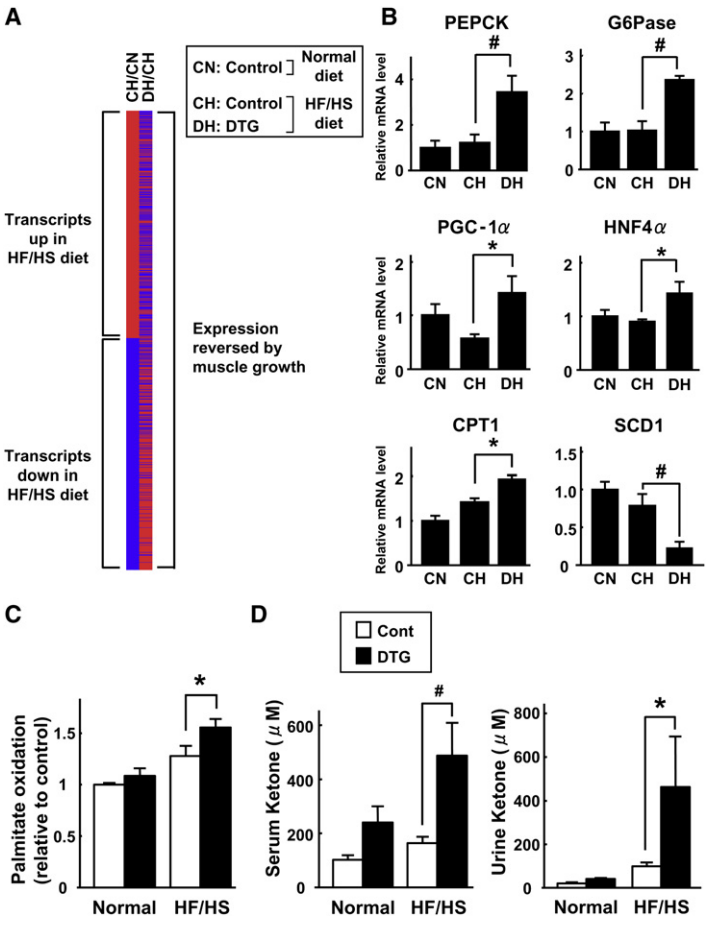

Figure 7. Akt1-Mediated Muscle Hypertrophy Promotes Fatty Acid Metabolism in Liver

(A) Comparison of transcripts significantly ($p < 0.05$) upregulated (red) or downregulated (blue) in liver under different experimental conditions ($n = 4$ in each group). Left column: comparison between control mice fed a HF/HS diet (CH) and control mice fed a normal diet (CN). Comparing these experimental conditions, 635 transcripts were upregulated and 646 transcripts were downregulated by the HF/HS diet. Right column: comparison between DTG mice fed a HF/HS diet (DH) and control mice fed a HF/HS diet (CH). 861 (67%) of the 1281 transcript expression changes in liver caused by the HF/HS diet were reversed by muscle growth.

(B) Relative mRNA expression levels of PEPCK, G6Pase, PGC-1α, HNF4α, CPT1, and SCD1 as measured by qRT-PCR in livers of control mice fed a normal diet (CN), control mice fed a HF/HS diet (CH), and DTG mice fed a HF/HS diet (DH) at the 3 week time point after DOX treatment ($n = 4$).

(C) Akt1-mediated muscle growth (3 weeks) promotes β-oxidation of palmitic acid in liver tissue ($n = 8$ in each group).

(D) Serum (left) and urine (right) ketone body levels in the different experimental groups of mice ($n = 9$–12 in each group). MCK-rtTA single-transgenic mice were used as a control.

Results are presented as mean ± SEM. *$p < 0.05$; #$p < 0.01$.

from the increase in glucose uptake by muscle, which leads the pancreas to secrete less insulin and more glucogen. These conditions would favor hepatic β-oxidation, ketogenesis, and gluconeogenesis and promote lipolysis in adipocytes. In addition, it is tempting to speculate that type II skeletal muscle allows the organism to cope with excess adipose tissue through the production of hormonal factors released by muscle that act on adipose, hepatic, or central nervous system tissues. As such, these muscle-secreted factors, or myokines (Pedersen et al., 2007), may oppose the actions of adipose-derived cytokines that promote metabolic disorders. However, the levels of IL-6, a myokine candidate, did not change upon muscle growth in our model, suggesting that other as yet unidentified factors produced by type IIb muscle coordinate these metabolic activities.

A number of parallels can be drawn between obese mice undergoing Akt1-mediated muscle growth and obese mice on a ketogenic diet. A ketogenic diet leads to reductions in body weight and fat-pad mass that are accompanied by an increase in energy expenditure (Kennedy et al., 2007). These effects are associated with reductions in insulin and leptin levels and numerous changes in the hepatic transcript expression profile, including a marked reduction in the expression of SCD1. Similar to *Akt1* transgenic mice, myostatin-deficient mice are resistant to the development of obesity, but these changes appear to occur independently of detectable changes in O_2 consumption and respiratory exchange ratio (McPherron and Lee, 2002). Surprisingly, administration of myostatin to mice leads to reductions in both muscle and fat mass (Zimmers et al., 2002), indicating that the regulation of fat mass by myostatin-mediated changes in muscle growth is complex and incompletely understood. Furthermore, a direct action of myostatin on adipose tissue has been reported (Feldman et al., 2006).

In summary, we have created a conditional transgenic mouse model that specifically expresses Akt1 in skeletal muscle, leading to functional type II skeletal muscle growth and regression in a sequential manner. In a model of diet-induced obesity, reversible Akt1-mediated type II muscle growth led to the reversible reduction of fat mass and overall body mass independent of changes in physical activity and food intake. Muscle growth also led to an improvement in whole-body metabolism that was associated with an increase in fatty acid β-oxidation in liver, the production of ketone bodies, and the resolution of hepatic steatosis. These

Figure 6. Akt1-Mediated Changes in Muscle Gene Expression

(A) Representative gene set enrichment analysis (GSEA) plots highlighting expression differences in gastrocnemius muscle after 3 weeks of *Akt1* transgene activation. Control and DTG mice were fed a HF/HS diet for 8 weeks prior to DOX treatment. Plots are shown for starch and sucrose metabolism, nuclear receptors, fatty acid metabolism, and oxidative phosphorylation gene sets (false discovery rate < 25%). Heat maps show the expression value differences for the top subset of genes that are represented in each gene set. Red corresponds to a high expression value; blue indicates a lower expression value ($n = 4$ in each group).

(B) Relative mRNA expression levels of PGC-1α, PPARα, PPARδ, hexokinase 2 (HK2), phosphofructokinase (Pfk), and lactate dehydrogenase A (LDHA) as measured by qRT-PCR.

(C) Relative protein expression levels of PGC-1α, PPARα, and PPARδ as determined by western blot analysis. MCK-rtTA single-transgenic mice were used as a control.

Results are presented as mean ± SEM. *$p < 0.05$.

changes in liver function were accompanied by marked changes in the expression of hepatic genes that control energy balance. The metabolic improvement in this model cannot be entirely explained by a reduction in fat-pad mass, indicating that type II muscle counteracts the actions of excess adipose tissue on whole-body metabolism. These findings indicate that type II muscle has a previously unappreciated role in regulating whole-body metabolism through its ability to alter the metabolic properties of remote tissues. These data also suggest that strength training, in addition to the widely prescribed therapy of endurance training, may be of particular benefit to overweight individuals.

EXPERIMENTAL PROCEDURES

Skeletal Muscle-Specific Conditional *Akt1* Transgenic Mice

1256 [3Emut] MCK-rtTA TG mice (Grill et al., 2003) were crossed with TRE-myrAkt1 TG mice (Shiojima et al., 2005) to generate double-TG (DTG) mice. For *Akt1* transgene expression, DTG mice were treated with DOX (0.5 mg/ml) in drinking water, and DOX water was removed to repress the transgene expression. 1256 [3Emut] MCK-rtTA TG littermates were used as controls and treated with DOX in the same manner as DTG mice.

Animal Care and Diet Treatments

Study protocols were approved by the Boston University Institutional Animal Care and Use Committee. Mice were fed either a normal chow diet (Harlan Teklad global 18% protein rodent diet, #2018) or a HF/HS diet (Bio-Serv, #F1850) (Harte et al., 1999) as indicated. The composition of the HF/HS diet was 35.8% fat (primarily lard), 36.8% carbohydrate (primarily sucrose), and 20.3% protein. Food consumption and body weight were monitored daily in individually caged mice. Rapamycin treatment was performed as described previously (Shioi et al., 2003).

Physiological Measurements

O_2 consumption, CO_2 production, and ambulatory activity levels were determined using a four-chamber Oxymax system (Columbus Instruments) with one mouse per chamber as described previously (Yu et al., 2000). Mice were monitored first for 24 hr under fed conditions and then for an additional 24 hr without food. Photo cells were aligned to the x, y, and z axes of the chambers to quantify habitual ambulatory activity. Forced treadmill exercise test was performed by using a treadmill (Columbus Instruments) as described previously (Arany et al., 2007). Following acclimation, muscle strength in mice was measured using an automated Grip Strength Meter (Columbus Instruments) as described previously (Acakpo-Satchivi et al., 1997).

MRI Measurements

MRI was performed on a Bruker Avance 500 wide-bore NMR spectrometer (11.7 T, or 500 MHz for proton) fitted with high-power gradient amplifiers for imaging (Viereck et al., 2005). Mice were sedated with 50–100 mg/kg ketamine administered intraperitoneally (i.p.) and restrained in an ergonomically designed cradle within the imaging coil. Twenty-four 1 mm thick axial slices were obtained spanning the abdomen using a RARE sequence. The following parameters were used: RARE factor = 8; $T\alpha$ = 8 ms; time of repetition [TR] = 2500 ms; field of view [FOV] = 25 mm; matrix size [MTX] = 256; total acquisition time $\sim$ 10 min.

Metabolic Measurements

Blood glucose was assayed with an Accu-Chek glucose monitor (Roche Diagnostics Corp.). Serum insulin levels were determined by ELISA using mouse insulin as a standard (Crystal Chem Inc.). Serum glucagon levels were measured by Glucagon EIA Kit (Cosmo Bio). Serum leptin levels were determined by mouse leptin ELISA (R&D Systems). Serum and urine ketone body levels were measured by Autokit Total Ketone Bodies (Wako). Serum lactate levels were determined by Lactate Assay Kit (BioVision).

Glucose tolerance testing was performed on 6 hr-fasted mice injected i.p. with D-glucose (1 g/kg body weight). Blood glucose levels were determined immediately before and 30, 60, 90, and 120 min after injection. Insulin tolerance testing was performed on 6 hr-fasted mice injected i.p. with human insulin (1.5 U/kg body weight, Humulin R, Eli Lilly). Blood glucose levels were determined immediately before and 20, 40, and 60 min after injection. Glucose uptake into skeletal muscle in vivo was determined as described previously (Koh et al., 2006). The rate of fatty acid β-oxidation in liver was examined as described previously (Nemoto et al., 2000).

Histology

Skeletal muscle and liver tissues were embedded in OCT compound (Sakura Finetech USA Inc.) and snap frozen in liquid nitrogen. WAT sections were fixed in 10% formalin, dehydrated, and embedded in paraffin. Tissue sections were stained with hematoxylin and eosin for overall morphology and oil red O for lipid deposition by standard methods. Fiber type staining was performed using MHC type I (BA-F8), MHC type IIa (SC-71), and MHC type IIb (BF-F3) monoclonal antibodies. The cross-sectional area of muscle fibers was determined using MetaMorph software.

Western Blotting

Western blot analysis was performed as described previously (Shiojima et al., 2002). Antibodies used were phospho-Akt (Ser473), phospho-p70 S6K, and Akt2 from Cell Signaling Technology; Akt1, VP16, and PPARδ from Santa Cruz Biotechnology, Inc.; PPARα from Abcam; HA (12CA5) from Roche Diagnostics; and PGC-1α and tubulin from Calbiochem.

Quantitative Real-Time PCR

Total RNA from whole gastrocnemius muscle and liver was prepared by QIAGEN RNeasy kit using manufacturer protocols. cDNA was produced using the ThermoScript RT-PCR System (Invitrogen). Real-time PCR was performed as described previously (Ouchi et al., 2005). Transcript levels were determined relative to the signal from 36B4 and normalized to the mean value of samples from control mice fed a normal diet. Primer sequences are listed in Table S1.

Microarray Analysis

Microarray analysis was carried out as described in detail previously (Schiekofer et al., 2006). Gene set enrichment analysis (GSEA) was performed to examine for sets of related genes that were altered in each experimental group (Lagouge et al., 2006).

Statistical Analysis

All data are presented as mean ± SEM. Statistical comparisons of data from two experimental groups were made using Student's t test. Comparisons of data from multiple groups were made by ANOVA with Fisher's protected least significant difference test.

Supplemental Data

Supplemental Data include Supplemental Experimental Procedures, Supplemental References, one table, and seven figures and can be found with this article online at http://www.cellmetabolism.org/cgi/content/full/7/2/159/DC1/.

ACKNOWLEDGMENTS

The authors thank D. Kelly, J. Breslow, and L. Goodyear for helpful advice.

Received: July 20, 2007
Revised: October 9, 2007
Accepted: November 5, 2007
Published: February 5, 2008

REFERENCES

Acakpo-Satchivi, L.J., Edelmann, W., Sartorius, C., Lu, B.D., Wahr, P.A., Watkins, S.C., Metzger, J.M., Leinwand, L., and Kucherlapati, R. (1997). Growth and muscle defects in mice lacking adult myosin heavy chain genes. J. Cell Biol. *139*, 1219–1229.

Albright, A., Franz, M., Hornsby, G., Kriska, A., Marrero, D., Ullrich, I., and Verity, L.S. (2000). American College of Sports Medicine position stand. Exercise and type 2 diabetes. Med. Sci. Sports Exerc. *32*, 1345–1360.

American Diabetes Association (2000). Diabetes mellitus and exercise. Diabetes Care *23* (*Suppl 1*), S50–S54.

Arany, Z., Lebrasseur, N., Morris, C., Smith, E., Yang, W., Ma, Y., Chin, S., and Spiegelman, B.M. (2007). The transcriptional coactivator PGC-1beta drives the formation of oxidative type IIX fibers in skeletal muscle. Cell Metab. *5*, 35–46.

Atherton, P.J., Babraj, J., Smith, K., Singh, J., Rennie, M.J., and Wackerhage, H. (2005). Selective activation of AMPK-PGC-1alpha or PKB-TSC2-mTOR signaling can explain specific adaptive responses to endurance or resistance training-like electrical muscle stimulation. FASEB J. *19*, 786–788.

Bodine, S.C., Stitt, T.N., Gonzalez, M., Kline, W.O., Stover, G.L., Bauerlein, R., Zlotchenko, E., Scrimgeour, A., Lawrence, J.C., Glass, D.J., and Yancopoulos, G.D. (2001). Akt/mTOR pathway is a crucial regulator of skeletal muscle hypertrophy and can prevent muscle atrophy in vivo. Nat. Cell Biol. *3*, 1014–1019.

Bolster, D.R., Kubica, N., Crozier, S.J., Williamson, D.L., Farrell, P.A., Kimball, S.R., and Jefferson, L.S. (2003). Immediate response of mammalian target of rapamycin (mTOR)-mediated signalling following acute resistance exercise in rat skeletal muscle. J. Physiol. *553*, 213–220.

Browning, J.D., and Horton, J.D. (2004). Molecular mediators of hepatic steatosis and liver injury. J. Clin. Invest. *114*, 147–152.

Cleasby, M.E., Reinten, T.A., Cooney, G.J., James, D.E., and Kraegen, E.W. (2007). Functional studies of Akt isoform specificity in skeletal muscle in vivo; maintained insulin sensitivity despite reduced insulin receptor substrate-1 expression. Mol. Endocrinol. *21*, 215–228.

Cohen, P., Miyazaki, M., Socci, N.D., Hagge-Greenberg, A., Liedtke, W., Soukas, A.A., Sharma, R., Hudgins, L.C., Ntambi, J.M., and Friedman, J.M. (2002). Role for stearoyl-CoA desaturase-1 in leptin-mediated weight loss. Science *297*, 240–243.

Dobrzyn, A., and Ntambi, J.M. (2005). The role of stearoyl-CoA desaturase in the control of metabolism. Prostaglandins Leukot. Essent. Fatty Acids *73*, 35–41.

Feldman, B.J., Streeper, R.S., Farese, R.V., Jr., and Yamamoto, K.R. (2006). Myostatin modulates adipogenesis to generate adipocytes with favorable metabolic effects. Proc. Natl. Acad. Sci. USA *103*, 15675–15680.

Grill, M.A., Bales, M.A., Fought, A.N., Rosburg, K.C., Munger, S.J., and Antin, P.B. (2003). Tetracycline-inducible system for regulation of skeletal muscle-specific gene expression in transgenic mice. Transgenic Res. *12*, 33–43.

Harris, T.E., and Lawrence, J.C., Jr. (2003). TOR signaling. Sci. STKE *2003*, re15.

Harte, R.A., Kirk, E.A., Rosenfeld, M.E., and LeBoeuf, R.C. (1999). Initiation of hyperinsulinemia and hyperleptinemia is diet dependent in C57BL/6 mice. Horm. Metab. Res. *31*, 570–575.

Hickson, R.C. (1980). Interference of strength development by simultaneously training for strength and endurance. Eur. J. Appl. Physiol. Occup. Physiol. *45*, 255–263.

Kennedy, A.R., Pissios, P., Otu, H., Xue, B., Asakura, K., Furukawa, N., Marino, F.E., Liu, F.F., Kahn, B.B., Libermann, T.A., and Maratos-Flier, E. (2007). A high-fat, ketogenic diet induces a unique metabolic state in mice. Am. J. Physiol. Endocrinol. Metab. *292*, E1724–E1739.

Koh, H.J., Arnolds, D.E., Fujii, N., Tran, T.T., Rogers, M.J., Jessen, N., Li, Y., Liew, C.W., Ho, R.C., Hirshman, M.F., et al. (2006). Skeletal muscle-selective knockout of LKB1 increases insulin sensitivity, improves glucose homeostasis, and decreases TRB3. Mol. Cell. Biol. *26*, 8217–8227.

Lagouge, M., Argmann, C., Gerhart-Hines, Z., Meziane, H., Lerin, C., Daussin, F., Messadeq, N., Milne, J., Lambert, P., Elliott, P., et al. (2006). Resveratrol improves mitochondrial function and protects against metabolic disease by activating SIRT1 and PGC-1alpha. Cell *127*, 1109–1122.

Lai, K.M., Gonzalez, M., Poueymirou, W.T., Kline, W.O., Na, E., Zlotchenko, E., Stitt, T.N., Economides, A.N., Yancopoulos, G.D., and Glass, D.J. (2004). Conditional activation of akt in adult skeletal muscle induces rapid hypertrophy. Mol. Cell. Biol. *24*, 9295–9304.

Leone, T.C., Lehman, J.J., Finck, B.N., Schaeffer, P.J., Wende, A.R., Boudina, S., Courtois, M., Wozniak, D.F., Sambandam, N., Bernal-Mizrachi, C., et al. (2005). PGC-1alpha deficiency causes multi-system energy metabolic derangements: muscle dysfunction, abnormal weight control and hepatic steatosis. PLoS Biol. *3*, e101.

Li, B., Nolte, L.A., Ju, J.S., Han, D.H., Coleman, T., Holloszy, J.O., and Semenkovich, C.F. (2000). Skeletal muscle respiratory uncoupling prevents diet-induced obesity and insulin resistance in mice. Nat. Med. *6*, 1115–1120.

Luquet, S., Lopez-Soriano, J., Holst, D., Fredenrich, A., Melki, J., Rassoulzadegan, M., and Grimaldi, P.A. (2003). Peroxisome proliferator-activated receptor delta controls muscle development and oxidative capability. FASEB J. *17*, 2299–2301.

McPherron, A.C., and Lee, S.J. (2002). Suppression of body fat accumulation in myostatin-deficient mice. J. Clin. Invest. *109*, 595–601.

McPherron, A.C., Lawler, A.M., and Lee, S.-J. (1997). Regulation of skeletal muscle mass in mice by a new TGF-β superfamily member. Nature *387*, 83–90.

Nader, G.A., and Esser, K.A. (2001). Intracellular signaling specificity in skeletal muscle in response to different modes of exercise. J. Appl. Physiol. *90*, 1936–1942.

Nemoto, Y., Toda, K., Ono, M., Fujikawa-Adachi, K., Saibara, T., Onishi, S., Enzan, H., Okada, T., and Shizuta, Y. (2000). Altered expression of fatty acid-metabolizing enzymes in aromatase-deficient mice. J. Clin. Invest. *105*, 1819–1825.

Ouchi, N., Shibata, R., and Walsh, K. (2005). AMP-activated protein kinase signaling stimulates VEGF expression and angiogenesis in skeletal muscle. Circ. Res. *96*, 838–846.

Pallafacchina, G., Calabria, E., Serrano, A.L., Kalhovde, J.M., and Schiaffino, S. (2002). A protein kinase B-dependent and rapamycin-sensitive pathway controls skeletal muscle growth but not fiber type specification. Proc. Natl. Acad. Sci. USA *99*, 9213–9218.

Pedersen, B.K., Akerstrom, T.C., Nielsen, A.R., and Fischer, C.P. (2007). Role of myokines in exercise and metabolism. J. Appl. Physiol. *103*, 1093–1098.

Phung, T.L., Ziv, K., Dabydeen, D., Eyiah-Mensah, G., Riveros, M., Perruzzi, C., Sun, J., Monahan-Earley, R.A., Shiojima, I., Nagy, J.A., et al. (2006). Pathological angiogenesis is induced by sustained Akt signaling and inhibited by rapamycin. Cancer Cell *10*, 159–170.

Reilly, M.P., and Rader, D.J. (2003). The metabolic syndrome: more than the sum of its parts? Circulation *108*, 1546–1551.

Reitman, M.L. (2002). Metabolic lessons from genetically lean mice. Annu. Rev. Nutr. *22*, 459–482.

Rommel, C., Bodine, S.C., Clarke, B.A., Rossman, R., Nunez, L., Stitt, T.N., Yancopoulos, G.D., and Glass, D.J. (2001). Mediation of IGF-1-induced skeletal myotube hypertrophy by PI(3)K/Akt/mTOR and PI(3)K/Akt/GSK3 pathways. Nat. Cell Biol. *3*, 1009–1013.

Ryder, J.W., Bassel-Duby, R., Olson, E.N., and Zierath, J.R. (2003). Skeletal muscle reprogramming by activation of calcineurin improves insulin action on metabolic pathways. J. Biol. Chem. *278*, 44298–44304.

Schiekofer, S., Shiojima, I., Sato, K., Galasso, G., Oshima, Y., and Walsh, K. (2006). Microarray analysis of Akt1 activation in transgenic mouse hearts reveals transcript expression profiles associated with compensatory hypertrophy and failure. Physiol. Genomics *27*, 156–170.

Shield, M.A., Haugen, H.S., Clegg, C.H., and Hauschka, S.D. (1996). E box sites and a proximal regulatory region of the muscle creatine kinase gene differentially regulate expression in diverse skeletal muscles and cardiac muscle of transgenic mice. Mol. Cell. Biol. *16*, 5058–5068.

Shioi, T., McMullen, J.R., Tarnavski, O., Converso, K., Sherwood, M.C., Manning, W.J., and Izumo, S. (2003). Rapamycin attenuates load-induced cardiac hypertrophy in mice. Circulation *107*, 1664–1670.

Shiojima, I., and Walsh, K. (2006). Regulation of cardiac growth and coronary angiogenesis by the Akt/PKB signaling pathway. Genes Dev. *20*, 3347–3365.

Shiojima, I., Yefremashvili, M., Luo, Z., Kureishi, Y., Takahashi, A., Tao, J., Rosenzweig, A., Kahn, C.R., Abel, E.D., and Walsh, K. (2002). Akt signaling mediates postnatal heart growth in response to insulin and nutritional status. J. Biol. Chem. *277*, 37670–37677.

Shiojima, I., Sato, K., Izumiya, Y., Schiekofer, S., Ito, M., Liao, R., Colucci, W.S., and Walsh, K. (2005). Disruption of coordinated cardiac hypertrophy

and angiogenesis contributes to the transition to heart failure. J. Clin. Invest. *115*, 2108–2118.

Takahashi, A., Kureishi, Y., Yang, J., Luo, Z., Guo, K., Mukhopadhyay, D., Ivashchenko, Y., Branellec, D., and Walsh, K. (2002). Myogenic Akt signaling regulates blood vessel recruitment during myofiber growth. Mol. Cell. Biol. *22*, 4803–4814.

Viereck, J., Ruberg, F.L., Qiao, Y., Perez, A.S., Detwiller, K., Johnstone, M., and Hamilton, J.A. (2005). MRI of atherothrombosis associated with plaque rupture. Arterioscler. Thromb. Vasc. Biol. *25*, 240–245.

Wang, Y.X., Zhang, C.L., Yu, R.T., Cho, H.K., Nelson, M.C., Bayuga-Ocampo, C.R., Ham, J., Kang, H., and Evans, R.M. (2004). Regulation of muscle fiber type and running endurance by PPARdelta. PLoS Biol. *2*, e294.

Williamson, D.L., Gallagher, P.M., Carroll, C.C., Raue, U., and Trappe, S.W. (2001). Reduction in hybrid single muscle fiber proportions with resistance training in humans. J. Appl. Physiol. *91*, 1955–1961.

Yu, S., Gavrilova, O., Chen, H., Lee, R., Liu, J., Pacak, K., Parlow, A.F., Quon, M.J., Reitman, M.L., and Weinstein, L.S. (2000). Paternal versus maternal transmission of a stimulatory G-protein alpha subunit knockout produces opposite effects on energy metabolism. J. Clin. Invest. *105*, 615–623.

Zierath, J.R., and Hawley, J.A. (2004). Skeletal muscle fiber type: influence on contractile and metabolic properties. PLoS Biol. *2*, e348.

Zimmers, T.A., Davies, M.V., Koniaris, L.G., Haynes, P., Esquela, A.F., Tomkinson, K.N., McPherron, A.C., Wolfman, N.M., and Lee, S.J. (2002). Induction of cachexia in mice by systemically administered myostatin. Science *296*, 1486–1488.

Accession Numbers

The microarray data discussed herein have been deposited in the NCBI Gene Expression Omnibus (http://www.ncbi.nih.gov/geo) with the accession number GSE9484.